Cell, Vol. 93, 1021–1029, June 12, 1998, Copyright ©1998 by Cell Press

Dynamin Undergoes a GTP-Dependent Conformational Change Causing Vesiculation

Sharon M. Sweitzer and Jenny E. Hinshaw*
Laboratory of Cell Biochemistry and Biology
National Institute of Diabetes and Digestive and Kidney Diseases
National Institutes of Health
Bethesda, Maryland 20892

Summary

The dynamin family of GTPases is essential for receptor-mediated endocytosis and synaptic vesicle recycling, and it has recently been shown to play a role in vesicle formation from the *trans*–Golgi network. Dynamin is believed to assemble around the necks of clathrin-coated pits and assist in pinching vesicles from the plasma membrane. This role would make dynamin unique among GTPases in its ability to act as a mechanochemical enzyme. Data presented here demonstrate that purified recombinant dynamin binds to a lipid bilayer in a regular pattern to form helical tubes that constrict and vesiculate upon GTP addition. This suggests that dynamin alone is sufficient for the formation of constricted necks of coated pits and supports the hypothesis that dynamin is the force-generating molecule responsible for membrane fission.

Introduction

Dynamin, a 100 kDa guanosine triphosphatase (GTPase), is essential for numerous intracellular membrane trafficking events. At the plasma membrane, the GTPase activity of dynamin is required for synaptic vesicle recycling (Kosaka and Ikeda, 1983), receptor-mediated endocytosis (see below), and caveolae internalization (Henley et al., 1998; Oh et al., 1998). Dynamin has been shown to be involved in the receptor-mediated endocytosis of transferrin and EGF receptors (Vieira et al., 1996), GLUT-4 (Omata et al., 1997; Volchuk et al. 1998; Al-Hasani et al., submitted), opioid receptors (Chu et al., 1997), and G protein–coupled receptors (Daaka et al., 1998). In addition, dynamin has recently been shown to be required for trafficking into and out of the Golgi complex (Jones et al., 1998; Llorente et al., 1998). Although it is clear that the GTPase activity of dynamin is required for the completion of these diverse processes, the specific role of dynamin remains unclear.

The dynamin family of GTPases consists of neuronal dynamin-1, ubiquitous dynamin-2, testes/neuronal dynamin-3, and a number of less closely related proteins (for review, see Urrutia et al., 1997). This family of proteins is distinguished from other GTPases by its high intrinsic GTPase activity and its low affinity for guanine nucleotides (for review, see Nuoffer and Balch, 1994; Warnock and Schmid, 1996). Dynamin also stimulates its own GTPase activity, resulting in a cooperative mechanism of activation (Tuma and Collins, 1994; Warnock et al., 1996). These unique properties have led to the speculation that dynamin is a force-generating molecular switch (Warnock and Schmid, 1996).

Dynamin was first shown to be involved in endocytosis with the discovery that it is the mammalian homolog to the *shibire* gene product in *Drosophila melanogaster* (Chen et al., 1991; Van der Bliek and Meyerowitz, 1991). *Drosophila* expressing the mutant *shibire*^{ts} gene product exhibit a rapid and reversible paralysis at the nonpermissive temperature (Poodry et al., 1973). Thin-section electron micrographs of the nerve termini from mutant flies reveal an absence of synaptic vesicles, an accumulation of coated pits at the plasma membrane, and electron dense collars surrounding the necks of these pits (Kosaka and Ikeda, 1983). This phenotype suggests that the *shibire* gene product is essential for membrane retrieval after neurotransmitter release. It was later demonstrated that overexpression of dominant-negative mutants of human dynamin-1 can effectively block clathrin-mediated endocytosis in mammalian cells, suggesting that the role of dynamin is conserved among eucaryotes (Van der Bliek et al., 1993).

The specific site of dynamin action was further elucidated by two simultaneous discoveries. Hinshaw and Schmid (1995) demonstrated that recombinant dynamin can self-assemble into spirals, and Takei et al. (1995) showed that GTPγS treatment of synaptosomes induced the formation of elongated membrane invaginations that were coated with the dynamin protein. These dynamin spirals and tubular invaginations both have dimensions similar to the proteinaceous structures seen at the necks of clathrin-coated pits in the *shibire* flies, leading to the speculation that dynamin assists in pinching the clathrin-coated pit from the plasma membrane. However, the hypothesis that dynamin acts as a "pinchase" has recently been challenged (Roos and Kelly, 1997).

Dynamin contains a number of conserved regions that may be important for its function, including an amino-terminal GTPase domain, a pleckstrin homology domain, a putative coiled-coil region, and a carboxyl-terminal proline-rich domain (PRD) (see Figure 2A and for review, Warnock and Schmid, 1996). The PRD of dynamin contains binding sites for src homology 3 (SH3) domain–containing proteins, which are thought to modulate the GTPase activity of dynamin (Gout et al., 1993; Herskovits et al., 1993) and to direct dynamin to the plasma membrane in vivo (Shpetner et al., 1996; Shupliakov et al., 1997). The PRD also has been implicated in dynamin binding to anionic phospholipids and lipid-mediated stimulation of the GTPase activity (Tuma et al., 1993), although conflicting data exist (Lin et al., 1997). SH3 domain–containing proteins are attractive candidates for regulators of dynamin function, since they bind to and activate the GTPase activity of dynamin in vitro; however, their role in vivo still remains unclear.

In addition to regulation by effector molecules, dynamin-1 may also be regulated by phosphorylation. Dynamin is phosphorylated in the PRD domain by protein

*To whom correspondence should be addressed.

kinase C (Robinson et al., 1993) and once phosphorylated is cytosolic (Liu et al., 1994a). The dephosphorylation of dynamin-1 by calcineurin temporally correlates with the depolarization of nerve termini and inhibits the GTPase activity of dynamin-1 (Liu et al., 1994b). The role of phosphorylation in the regulation of dynamin function remains unclear and may be specific to the nerve termini, since dynamin-2 appears not to be a substrate for protein kinase C (Sontag et al., 1994).

Until now, measuring dynamin function in vitro has been limited to assessing its GTPase activity. We report here a novel assay to investigate the role of dynamin in vesicle budding. Our data demonstrate that purified recombinant dynamin can bind to anionic phospholipids in the absence of other proteins or guanine nucleotides to form helical tubular structures. Treatment of these tubes with GTP causes a rapid alteration in structure, resulting in the constriction of dynamin tubes and the formation of numerous small vesicles. We believe that this represents a critical step in the process that occurs when clathrin-coated pits bud from the plasma membrane.

Results

Dynamin Binds to Lipid and Forms Helical Tubes

In the absence of any associated guanine nucleotide, purified recombinant dynamin-1 bound to phosphatidylserine liposomes and formed tubes as assessed by transmission electron microscopy (Figures 1A and 1B) and sedimentation (data not shown). Maximal binding was observed within 5 min at room temperature or on ice (data not shown). Analysis of computed diffraction patterns from the electron micrographs revealed that dynamin was bound to the lipid in a well-ordered helical lattice (Figure 1C). The dynamin tubes were approximately 50 nm in diameter, similar to the diameter of structures seen at the necks of clathrin-coated pits (Kosaka and Ikeda, 1983). Dynamin also bound to a crude lipid preparation from either clathrin-coated vesicles or total brain as well as to other anionic phospholipids, forming helical tubes similar to those described above, though not as abundant (data not shown).

The Proline-Rich Domain of Dynamin Is Not Required for Lipid Binding

To determine whether the PRD domain was necessary for tube formation, dynamin was digested with the protease subtilisin to remove its carboxyl terminus. The major proteolytic fragments (80, 40, and 15 kDa) of dynamin could be distinguished by using antibodies that recognize either the GTPase domain (α-dyn) or the PRD (hudy-1) (Figure 2A). Subtilisin-treated dynamin was incubated with lipid then subjected to centrifugation. Western analysis of the resultant supernates and pellets indicated that all proteolytic fragments were in the supernate in the absence of lipid (Figure 2B, lane 2). In the presence of lipid, amino-terminal fragments of dynamin were in the pellet, indicating that they bound to phosphatidylserine liposomes (Figure 2B, lane 5). The hudy-1 antibody, which recognizes the carboxyl-terminus of dynamin, did not recognize any peptides in the pellet fraction; all of the 15 kDa carboxyl-terminal peptide remained in the supernate (Figure 2B, lane 4). Once bound to lipid, the amino-terminal peptides of dynamin retained the ability to form tubes coated with a helical lattice of protein on the lipid surface (Figure 2C).

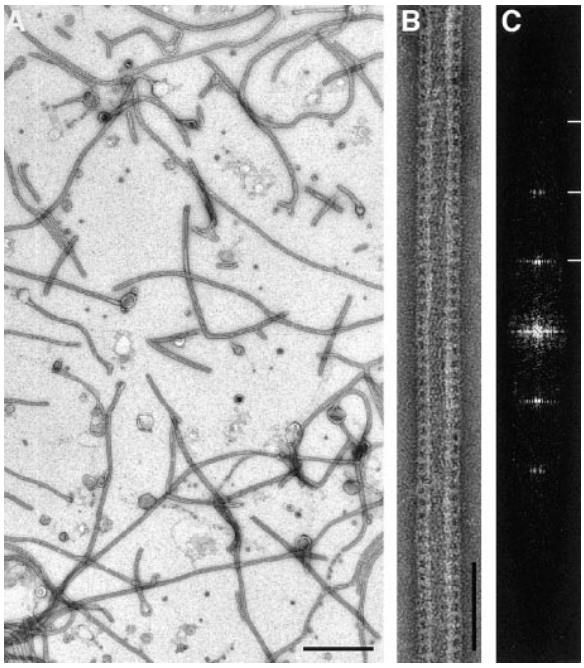

Figure 1. Dynamin Binds to Phosphatidylserine Liposomes and Forms Helical Tubes

(A) Low magnification electron micrograph of negatively stained dynamin tubes. Scale bar, 1 μm.

(B) As seen in this high magnification electron micrograph of a dynamin tube, spikes of dynamin extend $\sim$100 Å from the central lipid core ($\sim$300 Å in diameter) in the shape of a "T" and repeat every 132 Å up the tube. Vertical scale bar, 100 nm.

(C) The computed diffraction pattern of the average of two electron micrographs indicates that the tubes are well-ordered and helical. Hatch marks indicate layer lines at 1/132, 1/66, and 1/44 $Å^{-1}$.

The Proline-Rich Domain Is Accessible When Dynamin Is Bound to Lipid

To determine whether the carboxyl terminus of dynamin was accessible to effector molecules after dynamin was bound to lipid, we treated lipid-bound dynamin with the protease subtilisin. Subtilisin effectively removed the carboxyl terminus of dynamin, leaving the 80 kDa amino-terminal fragment bound to lipid (Figure 3A, lane 2). The removal of the carboxyl terminus was confirmed by Western analysis using the hudy-1 antibody (data not shown). Subtilisin treatment was also used to elucidate the region(s) of dynamin that interacts with the lipid bilayer. Extensive proteolysis (1 hr at room temperature) of dynamin in the absence of lipid resulted in a predominant 40 kDa fragment (Figure 3A, lane 1). The proteolytically sensitive region of dynamin, which contains the pleckstrin homology domain (Carr and Hinshaw, 1997; Muhlberg et al., 1997), was protected when dynamin was bound to lipid; only the carboxyl terminus was removed after extensive proteolysis (Figure 3A, lane 2).

The carboxyl terminus of dynamin was also accessible to protein kinase C, which was able to phosphorylate dynamin when it was bound to lipid (Figure 3D). Dynamin

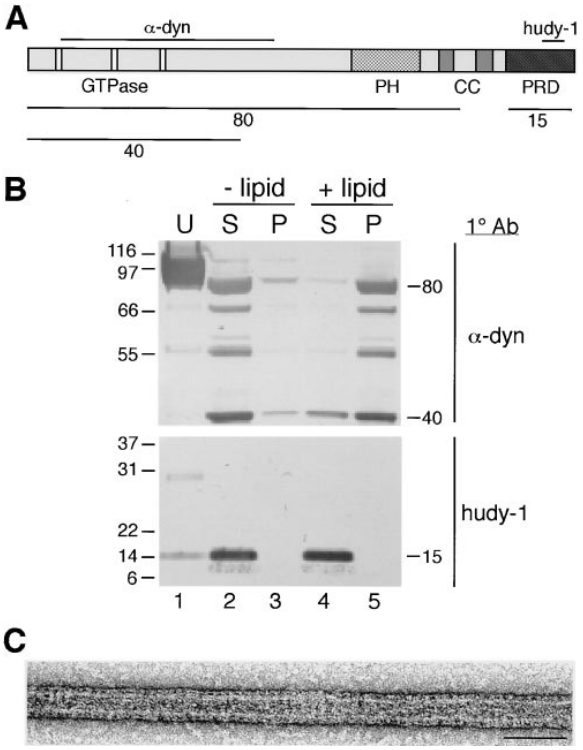

Figure 2. The Proline-Rich Domain of Dynamin Is Not Necessary for Lipid Binding

(A) Dynamin contains a tripartite GTPase domain (GTPase), a pleckstrin homology domain (PH), a putative coiled-coil region (CC), and a proline-rich domain (PRD). The approximate locations of the major proteolytic fragments and the regions recognized by the hudy-1 and α-dyn antibodies are indicated.

(B) Dynamin (lane 1; U, uncut) was treated with subtilisin for 1 hr on ice. The reaction was stopped, and the resultant fragments were incubated in the presence of lipid (lanes 4 and 5) or in the absence of lipid (lanes 2 and 3) and subjected to centrifugation. The supernates (S, lanes 2 and 4) and pellets (P, lanes 3 and 5) were subjected to SDS-PAGE and Western analysis. The resultant blot was cut in half above the 37 kDa molecular weight marker and analyzed with antibodies that recognize either the GTPase domain of dynamin (α-dyn, top) or the carboxyl-terminal proline-rich domain (hudy-1, bottom). hudy-1 did not react with any protein fragments in the pellet.

(C) Electron micrograph of a tube made from proteolyzed dynamin (~80 kDa) incubated with phosphatidylserine liposomes. Helical tubes are similar to those formed with full-length dynamin. Scale bar, 100 nm.

was prebound to phosphatidylserine liposomes, incubated with protein kinase C and ATP, and subjected to centrifugation to assess the amount of lipid-bound dynamin. Phosphorylation did not alter the total amount of dynamin that remained bound to lipid (compare Figures 3B [control] and 3C [phosphorylated]). The resultant autoradiogram shows dynamin that is bound to lipid is phosphorylated (Figure 3D). Proteolysis of phosphorylated dynamin with subtilisin confirmed that the phosphorylation site was on the 15 kDa carboxyl-terminal fragment (data not shown).

Dynamin Tubes Constrict and Vesiculate upon GTP Hydrolysis

Dynamin tubes provide a simple model system in which to address the role of GTP hydrolysis in vesiculation.

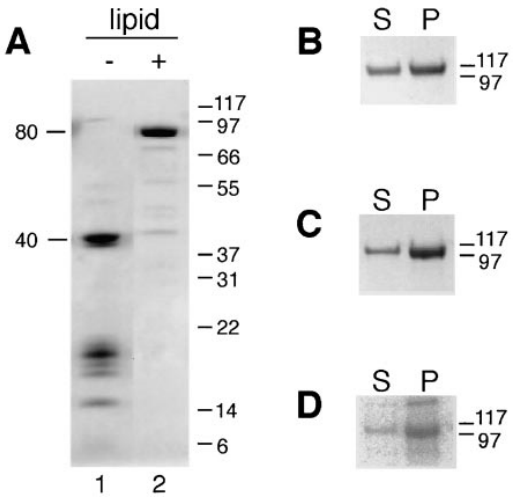

Figure 3. The Proline-Rich Domain of Dynamin Is Accessible to Effectors When Dynamin Is Bound to Lipid

(A) Dynamin was treated with subtilisin for 1 hr at room temperature (lane 1), or preformed dynamin tubes were treated with subtilisin for 1 hr at room temperature (lane 2). The resultant fragments were analyzed by SDS-PAGE and stained with Coomassie brilliant blue R.

(B–D) Dynamin tubes were formed and then incubated with either buffer alone (B) or buffer containing protein kinase C and ATP for 5 min at room temperature (C and D). The resultant mixture was subjected to sedimentation; supernates (S) and pellets (P) were analyzed by SDS-PAGE and transferred to nitrocellulose. Protein was detected by Ponceau S staining (B and C). Phosphorylation was detected by autoradiography (D).

Treatment of dynamin tubes with 1 mM GTP resulted in the rapid formation of numerous small dynamin-coated vesicles with a diameter of 60 ± 20 nm (Figures 4B and 4C). GTP treatment did not alter the ability of dynamin to bind to lipid as assessed by a sedimentation assay (data not shown). The few tubes remaining after GTP treatment were twisted, less permeable to stain, and constricted (of smaller diameter than untreated tubes) (Table 1, and compare Figures 4D and 4E), and they may represent an intermediate step in vesicle formation. The diameter of each tube remained constant along its length, suggesting a cooperative mechanism of constriction.

Vesiculation of dynamin tubes was also measured by light scattering; a reduction in light scattering consistently correlated with the vesiculation of tubes as seen by electron microscopy. Treatment of tubes with GTP resulted in a rapid and significant decrease in light scattering (Figure 5A). A similar drop in light scattering was detected after tubes were treated with either 1 mM or 100 μM GTP (Figure 5A). Treatment with 10 μM GTP resulted in a significant drop in light scattering with a slight recovery. These results are consistent with reported affinities of dynamin for GTP (34 μM, Tuma and Collins, 1994). GTP hydrolysis was necessary for vesiculation since other nucleotides (ATP or GDP) or nonhydrolyzable analogs of GTP (GTPγS or GMP-PCP) did not affect light scattering (Figure 5B). Binding of the nonhydrolyzable GTP analogs by dynamin was assessed by their ability to competitively inhibit vesiculation when additional GTP was added. K44A, a GTP binding mutant of dynamin (Van der Bliek et al., 1993), also formed tubes but was unable to mediate vesiculation (Figure 5B).

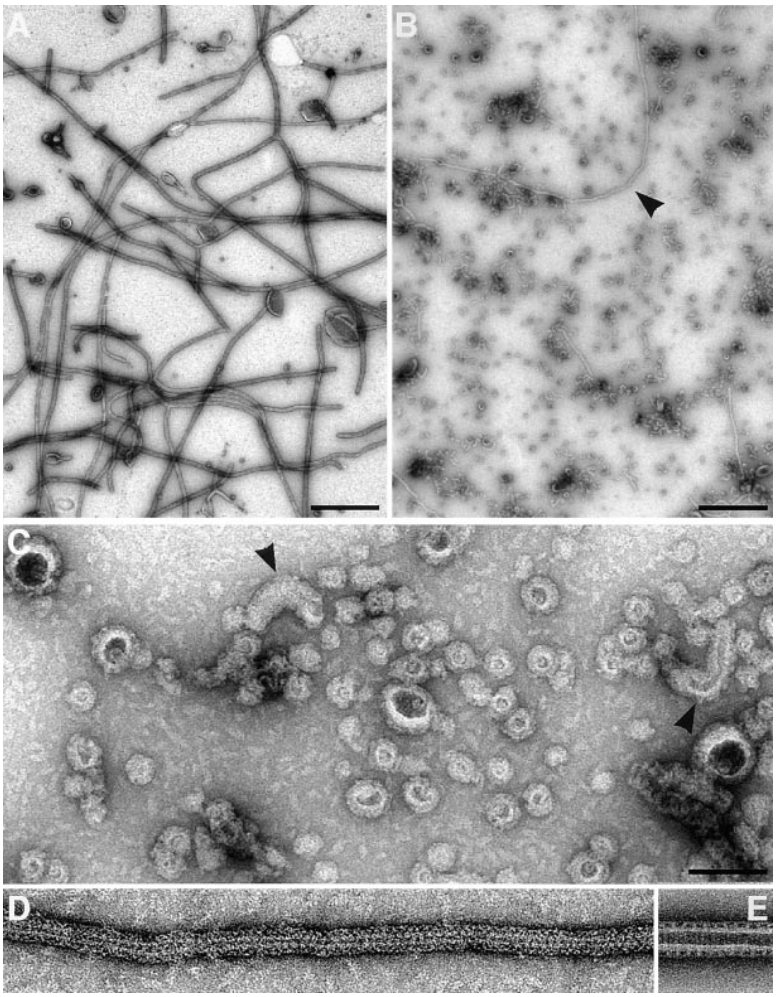

Figure 4. Treatment of Dynamin Tubes with GTP Causes a Major Structural Change

(A and B) Electron micrograph of negatively stained dynamin tubes that were treated for 5 min at room temperature with either buffer (A) or buffer containing 1 mM GTP (B). Arrowhead indicates a tube remaining after treatment. Scale bars, 1 μm.

(C) High magnification of small dynamin-coated vesicles formed after treatment. Arrowheads indicate small curved tube remnants. Scale bar, 100 nm.

(D and E) Comparison between a constricted tube resulting from GTP treatment (~40 nm in diameter [D]) and an untreated dynamin tube (~50 nm in diameter [E]). Same scale for (C)–(E).

The Proline-Rich Domain of Dynamin Is Not Necessary for Constriction and Vesiculation

Dynamin tubes were subjected to proteolysis by subtilisin to quantitatively remove the proline-rich domain. The resultant tubes were treated with either buffer alone (Figure 6A) or buffer containing 1 mM GTP (Figure 6B) for 5 min at room temperature. Similar tubes were assayed for vesiculation by light scattering (Figure 6C). Treatment with 1 mM GTP (arrowhead) resulted in a rapid drop in light scattering similar to the one seen with full-length dynamin.

Cryo-Electron Microscopy of Dynamin Tube Formation

Dynamin and liposomes were incubated for a brief time and then examined by cryo-electron microscopy to capture newly forming tubes. As seen in Figure 7, several structures may represent possible stages in tube formation. This process appears cooperative, considering that extended well-decorated dynamin tubes and partially decorated liposomes are present simultaneously (Figures 7A, 7B, and 7C). It is also apparent that the majority of the liposomes are unilamellar.

Table 1. Dynamin-Lipid Tubes Constrict upon GTP Treatment

	Control	1 mM GTP
Average tube diameter (nm)	52 ± 4 (N = 53)	43 ± 2 (N = 63)

Discussion

In the current study, we demonstrate that dynamin assembly on a lipid bilayer does not require integral membrane proteins, cytosolic factors, or guanine nucleotides. Dynamin alone can bind to a lipid bilayer, organize as a helical lattice, and form elongated tubular structures. These structures resemble the membrane invaginations of GTPγS-treated synaptosomes and have the same diameter as the structures seen at the necks of clathrin-coated pits in *shibire* flies (Kosaka and Ikeda, 1983). These similarities are more apparent when the dynamin tubes are examined by cryo-electron microscopy (Figure 7). Visualizing tubes in ice also gives us some insight into the mechanism of tube formation (Figures 7A–7C). It appears that dynamin assembly is cooperative; once initiated, tubes elongate readily.

In the absence of lipid, dynamin can assemble into helical spirals either in low salt (Hinshaw and Schmid, 1995) or in the presence of transition-state analogs of

GTP (Carr and Hinshaw, 1997). However, dynamin-lipid tubes form under conditions that do not favor spiral formation (100 mM salt and no GTP analogs). Treatment of preformed tubes with Triton X-100 results in structures that appear similar to dynamin spirals formed in the absence of lipid (data not shown). These results suggest that certain lipids may provide a surface on which dynamin–dynamin interactions occur readily, thereby shifting the equilibrium toward dynamin assembly. The self-association of membrane-bound dynamin may be responsible for the formation and stabilization of the neck of the coated pit in vivo, analogous to the way the clathrin lattice stabilizes curvature of the plasma membrane. However, unlike clathrin (Robinson, 1992), dynamin does not appear to require adaptor proteins for assembly on a membrane.

Phosphorylated dynamin retained the ability to form dynamin-lipid tubes in vitro. We propose that the PRD and the phosphorylation state of dynamin may be critical for recruitment of dynamin to the coated pits but are not involved in lipid association or helical assembly once dynamin is appropriately targeted. Since the carboxyl-terminal cleavage site was readily available to protease and membrane-associated dynamin could be phosphorylated by PKC, the PRD is likely to be accessible to SH3 domain–containing proteins and protein kinases when dynamin is bound to the plasma membrane. Another domain of dynamin that is a likely candidate for lipid binding is the pleckstrin homology domain (Zheng et al., 1996). In support of this, we found that the 40 kDa subtilisin-cleaved fragment, which was derived from the amino-terminal GTPase domain and therefore lacked the pleckstrin homology domain, did not bind to lipid (data not shown). In the future, overexpression and purification of dynamin fragments will help define the domain that is responsible for lipid binding.

Considering dynamin-lipid tubes resemble collars and tubular structures seen in vivo, they provide an ideal system to assess the effects of guanine nucleotide binding and hydrolysis on vesiculation. Our data show that, once bound to a lipid bilayer, dynamin alone can mediate constriction and vesiculation of membranes upon treatment with GTP. Vesiculation could be monitored either by electron microscopy, which demonstrated that the resultant vesicles remained coated with dynamin, or by light scattering, which demonstrated the rapid nature of this reaction. By both methods we determined that neither GTP analogs nor other nucleotides could induce vesiculation. We therefore conclude that GTP hydrolysis is responsible for vesiculation of dynamin tubes in vitro and that the carboxyl-terminal PRD domain of dynamin is not required for this process.

Our results also show that the dynamin tubes remaining after GTP treatment were consistently constricted (they were of smaller diameter than control tubes). It is tempting to speculate that the constricted tubes we see are related to the functionally defined constricted necks of clathrin-coated pits, which are defined by their ability to exclude avidin (Carter et al., 1993). Our untreated dynamin tubes have an aqueous channel at their centers, which appears to be ~200 Å in diameter, large enough to accommodate an avidin molecule (unit cell: a = 72.15 Å, b = 80.37 Å, c = 43.54 Å) (Livnah et al., 1993). The aqueous channel of the GTP-treated tubes appears to be ~70 Å, which may be small enough to exclude avidin. Our data then agree with experiments done in vivo which suggest that GTP is required for constriction of the necks of clathrin-coated pits. However, in contrast to these results, we do not see constricted tubes with the addition of GTPγS.

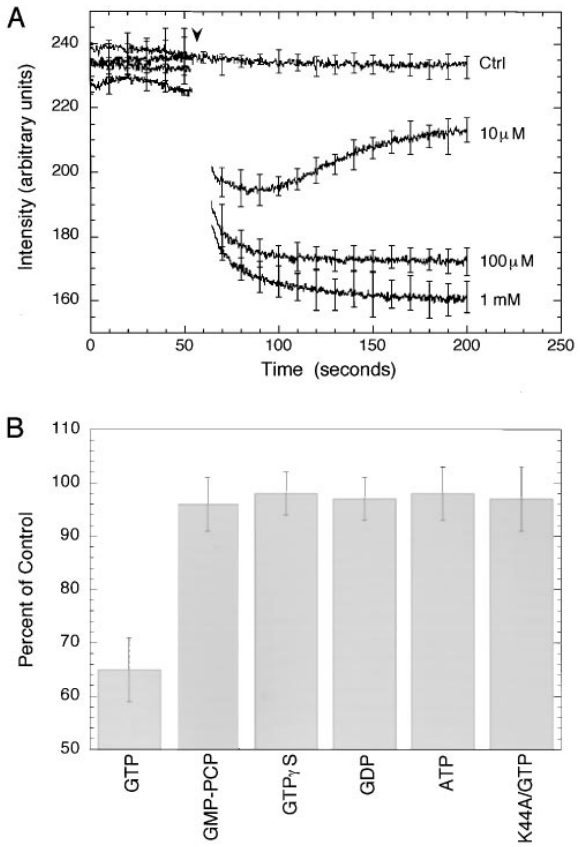

Figure 5. Light Scattering Confirms that Vesiculation Occurs Rapidly and Requires GTP Hydrolysis

(A) Time course of treatment with either 0 (ctrl), 10 μM, 100 μM, or 1 mM GTP as indicated. The data are an average of three experiments. Arrowhead indicates time of GTP addition.

(B) The drop in light scattering after 1 min of treatment is expressed as a percentage of the initial light scattering. Wild-type dynamin tubes were treated with either 1 mM GTP, GTPγS, GMP-PCP, GDP, or ATP. Only addition of GTP resulted in a significant decrease in light scattering. Dynamin tubes formed with the GTP binding mutant of dynamin (K44A) were treated with 1 mM GTP.

Dynamin is unique among GTPases, owing to its high intrinsic GTPase activity. In addition, pretreatment of dynamin tubes with 1 mM GDP had no effect on the subsequent vesiculation induced by 200 μM GTP (data not shown), suggesting that dynamin may not require a guanine nucleotide exchange factor for its activity. Other GTPases appear to work as molecular switches with the GTP-bound state being "on" and the GDP-bound state being "off." Our current work suggests that dynamin may not behave in this manner. Treatment of classical GTPases with GTP analogs can mimic either their on or off state. GTP binding is not sufficient to induce dynamin-mediated constriction and vesiculation; GTP hydrolysis is required. The constriction of GTP-treated

tubes also suggests that dynamin is a mechanochemical enzyme, where hydrolysis of GTP causes a dramatic conformational change that squeezes the lipid bilayer. We therefore conclude that dynamin does not behave as a molecular switch but as a force-generating molecule. Preliminary results indicate that recombinant dynamin-2 (Warnock et al., 1997), which shares a 79% amino acid identity with dynamin-1 (Cook et al., 1994; Warnock et al., 1997), can also form tubes that undergo a similar conformational change upon treatment with GTP (data not shown). This suggests that the process may be a general property of the dynamin family (for review, see Urrutia et al., 1997). This GTP-induced vesiculation has further significance with the recent discovery that dynamin-2 also plays a role at the Golgi apparatus (Jones et al., 1998).

Dynamin can cause vesiculation in vitro at nucleotide concentrations similar to intracellular GTP levels, indicating that dynamin would be fully capable of vesiculation under normal physiological conditions. Therefore, there may be an inhibitor of dynamin action that would regulate vesicle formation. Alternatively, dynamin may be unregulated, with the limiting step being the closure of the collar around the neck of the clathrin-coated pit. As soon as the collar is in place, vesiculation would occur. The inability of many investigators to visualize dynamin collars around the necks of clathrin-coated pits may then be explained by this rapid vesiculation event.

How does dynamin mediate vesiculation? In agreement with other groups, we propose that dynamin is recruited to the clathrin-coated pit via interactions with its proline-rich domain (Shpetner et al., 1996; Shupliakov et al., 1997). Once dynamin is appropriately targeted, it binds directly to the lipid bilayer, where dynamin–dynamin interactions drive the constriction of the bilayer into a tube, introducing strain into the membrane. GTP hydrolysis causes a further constriction of the dynamin helix around the tube, which may be sufficient for vesiculation. Alternatively, disruption of dynamin–dynamin interactions, which would result in a dramatic release of constraint on the membrane, may facilitate membrane fission. In addition, the affinity of dynamin for anionic phospholipids may recruit these fusagenic lipids to the neck of the clathrin-coated pit and thus alter the local lipid composition to favor vesiculation. Although it is clear that other proteins are necessary for vesicle formation and regulation in vivo, the evidence presented here shows that purified dynamin can act alone to cause membrane fission.

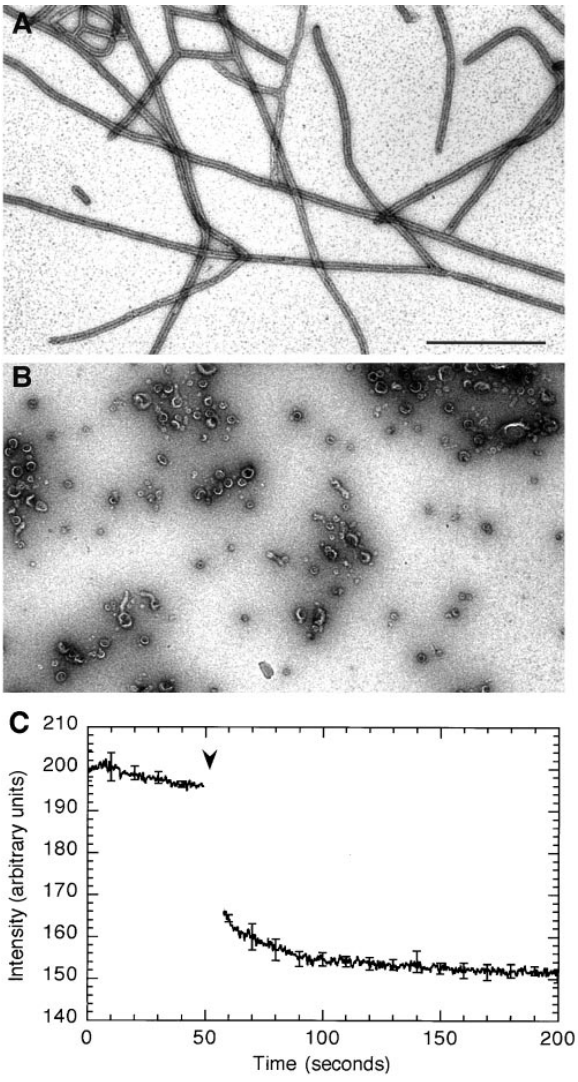

Figure 6. Dynamin Tubes that Were Subjected to Proteolysis with Subtilisin Were Capable of GTP-Induced Vesiculation

Subtilisin-treated dynamin tubes were treated for 5 min at room temperature with either (A) HCB100 or (B) 1 mM GTP in HCB100. Same scale for (A) and (B); scale bar, 1 μm. (C) Light scattering time course of subtilisin-treated dynamin tubes treated with 1 mM GTP. Arrowhead indicates time of GTP addition.

Experimental Procedures

Dynamin Tube Formation

Dynamin-1 and K44A were expressed in baculovirus-infected *TN5-JE* cells and purified as previously described (Warnock et al., 1996). The fraction of dynamin-1 bound to guanine nucleotide was determined to be less than 3% by HPLC (data not shown). Synthetic phosphatidylserine (0.5 mg 1,2-Dioleoyl-sn-glycero-3-[phospho-L-serine] [Avanti]) in HCB100 (20 mM HEPES [pH 7.2], 1 mM $MgCl_2$, 2 mM EGTA, 1 mM DTT, 1 mM PMSF, complete protease inhibitors [Calbiochem], 100 mM NaCl) was extruded 11 times through a 1 μm polycarbonate membrane (Avanti) to form unilamellar vesicles. Large vesicles were separated from smaller vesicles on a Sephacryl S-1000 column (Pharmacia Biotech) (average size: 155 ± 70 nm). Purified dynamin was diluted to 0.25 mg/ml protein and 100 mM KH_2PO_4 with HCB0 (HCB100 without NaCl). Dynamin was titrated against the lipid vesicles to achieve conditions where 50% of the dynamin was bound. Dynamin (0.25 mg/ml) and the appropriate concentrations of lipid were incubated at 20°C for 24–30 hr. For negative stained images, dynamin tubes were diluted 1:1 with HCB100, adsorbed to EM grids, washed with HCB0, and stained with 2% uranyl acetate. Similar tubes were made with dynamin-2 (protein generously provided by D. Warnock and S. Schmid) (Warnock et al., 1997) and K44A (baculovirus stock generously provided by D. Warnock and S. Schmid) (Warnock et al., 1996). For cryo-electron microscopy, dynamin tubes were adsorbed to holey grids, blotted, plunged into liquid ethane, and stored under liquid nitrogen prior to examination by transmission electron microscopy.

Proteolysis, Sedimentation, and Western Analysis

For experiments in Figure 2, purified dynamin was treated with 1:400 (wt:wt) subtilisin for 1 hr on ice and the reaction stopped by the

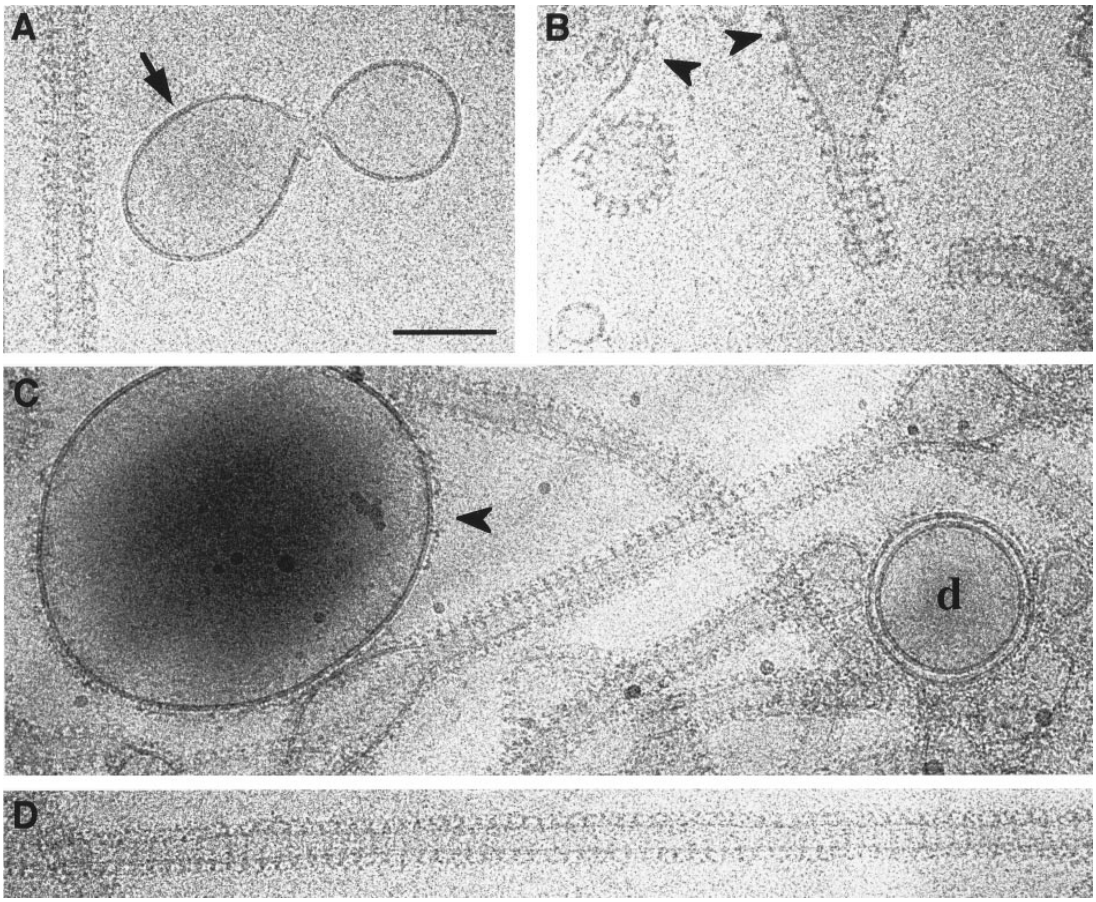

Figure 7. Dynamin Tube Formation Observed by Cryo-Electron Microscopy

Dynamin tubes were formed at 37°C for 1 hr, frozen in liquid ethane, and visualized by cryo-electron microscopy.

(A) In the center of the panel, a dynamin ring appears to be constricting a unilamellar vesicle. Arrow indicates a region of the lipid bilayer that is not decorated with dynamin.

(B) In the top center of the panel, a dynamin-coated tube can be seen forming from a large vesicle. The "T"-like shape of dynamin is clearly visible on the vesicle seen at the left. Arrowheads indicate partially decorated lipid bilayers.

(C) Structures seen in this panel are likely to represent the numerous stages of tube formation. Arrowhead indicates a large vesicle that is sparsely decorated with dynamin. This may represent an early stage in tube formation, since at later times few large vesicles are apparent (see Figures 1A and 4A). A smaller vesicle with a double lipid membrane (d) can also be seen. As expected, the inner membrane lacks any dynamin decoration.

(D) Elongated tube that is evenly coated with a helical lattice of dynamin, similar to those seen previously by negative stain (see Figure 1B). Same scale for (A)–(D); scale bar, 100 nm.

addition of 2 mM PMSF (Sigma). The resultant peptides were incubated either with or without phosphatidylserine vesicles for 1 hr at 37°C (maximal lipid binding was achieved within 5 min) and were subjected to centrifugation for 10 min at 436,000 × g (Figure 2B). For experiments in Figure 3, purified dynamin was incubated either with or without phosphatidylserine vesicles for 18 hr at 20°C and then treated with 1:400 (wt:wt) subtilisin for 1 hr at room temperature.

Proteins were run on a Nupage 4%–12% gel (Novex) and either stained with Coomassie brilliant blue R (Sigma) (Figure 3A) or transferred to nitrocellulose (Schleicher and Schuell) (Figure 2B). The resulting blot was cut in half at the 37 kDa molecular weight marker, and proteins were crosslinked to blot with 0.2% glutaraldehyde. The top of the blot was treated with primary antibodies against the GTPase domain of dynamin (α-dyn) (Signal Transduction Labs), and the bottom of the blot was treated with the hudy-1 antibody, which recognizes the PRD of dynamin (generously provided by S. Schmid). The secondary antibody, a goat anti-mouse IgG (Fab specific) alkaline phosphatase conjugate (Sigma), was detected using BCIP/NBT (Kirkegaard and Perry Laboratories).

Phosphorylation

Dynamin tubes were formed as described above except that lipid was made in HCB150 (150 mM NaCl) and used at concentrations sufficient to bind most detectable dynamin, which was diluted to 0.675 mg/ml protein and 150 mM salt. Dynamin tubes were incubated with either buffer (HCB0 containing 150 mM NaCl, and an additional 1.7 mM EGTA and 17 mM $MgCl_2$) or buffer containing PKC (Calbiochem) and γ^{32}P-ATP (Amersham) for 5 min at 37°C. Resultant phosphorylated dynamin was subjected to centrifugation as described above, and the supernates and pellets were analyzed by SDS-PAGE, transferred to nitrocellulose, stained with Ponceau S (Sigma), and exposed to a BAS-IIIs imaging plate (Fugi Photo Film Co.) for ~20 hr.

GTP Treatment

Dynamin tubes were formed as described above, adsorbed to carbon-coated EM grids for 5 min at room temperature, and treated with either HCB100 or HCB100 containing 1 mM GTP. After treatment,

samples were washed twice in HCB0 and stained with 2% uranyl acetate.

Light Scattering

90° light scattering was measured on an LS-50B spectrofluorometer (Perkin Elmer) at 350 nm with a 4% screen on the excitation. Excitation and emission slit widths were set at 5 nm. Measurements were made at 0.1 s intervals for 200 s. Dynamin tubes were prepared as described above and diluted 1:10 with HCB100. The indicated amounts of guanine nucleotides were added and gently mixed at ~1 min after measurements began. Measurements were averaged after ~1 min of treatment for an additional ~20 s. Reported values in Figure 5B are end point measurements expressed as a percent of initial measurements (averaged over ~50 s). The data are an average of at least three independent experiments.

Electron Microscopy and Image Analysis

Images were collected using a Philips CM120 transmission electron microscope at 100 keV. Electron micrographs were converted to digital images using a Leafscan 45 (Leaf Systems), and the diffraction patterns were computed using the SUPRIM software package (Schroeter and Bretaudiere, 1996) on an Indigo 2 SGI (Silicon Graphics).

Acknowledgments

The authors would like to acknowledge J. Carr for assistance with proteolysis experiments and electron microscopy, N. Peffley for experiments with clathrin-coated vesicles, Dr. D. Sackett for help with light scattering experiments, Dr. L. Green for clathrin-coated vesicles and HPLC analyses, and Dr. S. Schmid and Dr. D. Warnock for hudy-1 antibodies, dynamin-2 protein, and baculovirus stocks expressing dynamin-1 and K44A.

The authors would also like to acknowledge Dr. J. Hanover, Dr. R. Milligan, and Dr. S. Schmid for their continuous support, as well as M. Whittaker, Dr. J. Jontes, and Dr. D. Warnock for their initial help with the lipid studies; and J. Carr, Dr. G. Ashwell, Dr. J. Hanover, Dr. A. Robbins, Dr. D. Sackett, Dr. T. Sweitzer, and Dr. H. Wein for critical reading of the manuscript.

Received March 18, 1998; revised April 27, 1998.

References

Carr, J.F., and Hinshaw, J.E. (1997). Dynamin assembles into spirals under physiological salt conditions upon the addition of GDP and γ-phosphate analogues. J. Biol. Chem. *272*, 28030–28035.

Carter, L.L., Redelmeier, T.E., Woollenweber, L.A., and Schmid, S.L. (1993). Multiple GTP-binding proteins participate in clathrin-coated vesicle-mediated endocytosis. J. Cell Biol. *120*, 37–45.

Chen, M.S., Obar, R.A., Schroeder, C.C., Austin, T.W., Poodry, C.A., Wadsworth, S.C., and Vallee, R.B. (1991). Multiple forms of dynamin are encoded by *shibire*, a Drosophila gene involved in endocytosis. Nature *351*, 583–586.

Chu, P., Murray, S., Lissin, D., von Zastrow, M. (1997). δ and κ opioid receptors are differentially regulated by dynamin-dependent endocytosis when activated by the same alkaloid agonist. J. Biol. Chem. *272*, 27124–27130.

Cook, T.A., Urrutia, R., and McNiven, M.A. (1994). Identification of dynamin 2, an isoform ubiquitously expressed in rat tissues. Proc. Natl. Acad. Sci. USA *91*, 644–648.

Daaka, Y., Luttrell, L.M., Ahn, S., Della Roca, G.J., Ferguson, S.S.G., Caron, M.G., and Lefkowitz, R.J. (1998). Essential role for G protein-coupled receptor endocytosis in the activation of mitogen-activated protein kinase. J. Biol. Chem. *273*, 685–688.

Gout, I., Dhand, R., Hiles, I.D., Fry, M.J., Panayotou, G., Das, P., Truong, O., Totty, N.F., Hsuan, J., Booker, G.W., Campbell, I.D., and Waterfield, M.D. (1993). The GTPase dynamin binds to and is activated by a subset of SH3 domains. Cell *75*, 25–36.

Henley, J.R., Krueger, E.W.A., Oswald, B.J., and McNiven, M.A. (1998). Dynamin-mediated internalization of caveolae. J. Cell. Biol. *141*, 85–99.

Herskovits, J.S., Shpetner, H.S., Burgess, C.C., and Vallee, R.B. (1993). Microtubules and Src homology 3 domains stimulate the dynamin GTPase via its C-terminal domain. Proc. Natl. Acad. Sci. USA *90*, 11468–11472.

Hinshaw, J.E., and Schmid, S.L. (1995). Dynamin self-assembles into rings suggesting a mechanism for coated vesicle budding. Nature *374*, 190–192.

Jones, S.M., Howell, K.E., Henley, J.R., Cao, H., and McNiven, M.A. (1998). Role of dynamin in the formation of transport vesicles from the trans-golgi network. Science *279*, 573–577.

Kosaka, T., and Ikeda, K. (1983). Possible temperature-dependent blockage of synaptic vesicle recycling induced by a single gene mutation in Drosophila. J. Neurobiol. *14*, 207–225.

Lin, H.C., Barylko, B., Achiriloaie, M., and Albanesi, J.P. (1997). Phosphatidylinositol (4,5)-bisphosphate-dependent activation of dynamins I and II lacking the proline/arginine-rich domains. J. Biol. Chem. *272*, 25999–26004.

Liu, J.-P., Powell, K.A., Südhof, T.C., and Robinson, P.J. (1994a). Dynamin I is a Ca^{2+}-sensitive phospholipid-binding protein with very high affinity for protein kinase C. J. Biol. Chem. *269*, 21043–21050.

Liu, J.-P., Sim, A.T.R., and Robinson, P.J. (1994b). Calcineurin inhibition of dynamin I GTPase activity coupled to nerve terminal depolarization. Science *265*, 970–973.

Livnah, O., Bayer, E.A., Wilchek, M., and Sussman, J.L. (1993). Three-dimensional structures of avidin and the avidin-biotin complex. Proc. Natl. Acad. Sci. USA *90*, 5076–5080.

Llorente, A., Rapak, A., Schmid, S.L., van Deurs, B., and Sandvig, K. (1998). Expression of mutant dynamin inhibits toxicity and transport of endocytosed ricin to the Golgi apparatus. J. Cell Biol. *140*, 553–563.

Muhlberg, A.B., Warnock, D.E., and Schmid, S.L. (1997). Domain structure and intra-molecular regulation of dynamin GTPase. EMBO J. *16*, 6676–6683.

Nuoffer, C., and Balch, W.E. (1994). GTPases: multifunctional molecular switches regulating vesicular traffic. Annu. Rev. Biochem. *63*, 949–990.

Oh, P., McIntosh, D.P., and Schnitzer, J.E. (1998). Dynamin at the neck of caveolae mediates their budding to form transport vesicles by GTP-driven fission from the plasma membrane. J. Cell Biol. *141*, 101–114.

Omata, W., Shibata, H., Suzuki, Y., Tanaka, S., Suzuki, T., Takata, K., and Kojima, I. (1997). Subcellular distribution of GLUT4 in Chinese hamster ovary cells overexpressing mutant dynamin: evidence that dynamin is a regulatory GTPase in GLUT4 endocytosis. Biochem. Biophys. Res. Comm. *241*, 401–406.

Poodry, C.A., Hall, L., and Suzuki, D.T. (1973). Developmental properties of *shibire*^{ts1}: a pleiotropic mutation affecting larval and adult locomotion and development. Dev. Biol. *32*, 373–386.

Robinson, M.S. (1992). Adaptins. Trends Cell. Biol. *2*, 293–297.

Robinson, P.J., Sontag, J.-M., Liu, J.-P., Fykse, E.M., Slaughter, C., McMahon, H., and Südhof, T.C. (1993). Dynamin GTPase regulated by protein kinase C phosphorylation in nerve terminals. Nature *365*, 163–166.

Roos, J., and Kelly, R.B. (1997). Is dynamin really a "pinchase"? Trends Cell. Biol. *7*, 257–259.

Schroeter, J.P., and Bretaudiere, J.-P. (1996). SUPRIM: easily modified image processing software. J. Struct. Biol. *116*, 131–137.

Shpetner, H.S., Herskovits, J.S., and Vallee, R.B. (1996). A binding site for SH3 domains targets dynamin to coated pits. J. Biol. Chem. *271*, 13–16.

Shupliakov, O., Löw, P., Grabs, D., Gad, H., Chen, H., David, C., Takei, K., De Camilli, P., and Brodin, L. (1997). Synaptic vesicle endocytosis impaired by disruption of dynamin-SH3 domain interactions. Science *276*, 259–263.

Sontag, J.-M., Fykse, E.M., Ushkaryov, Y., Liu, J.-P., Robinson, P.J., and Südhof, T.C. (1994). Differential expression and regulation of multiple dynamins. J. Biol. Chem. *269*, 4547–4554.

Takei, K., McPherson, P.S., Schmid, S.L., and De Camilli, P. (1995). Tubular membrane invaginations coated by dynamin rings are induced by GTP-γS in nerve terminals. Nature *374*, 186–190.

Tuma, P.L., and Collins, C.A. (1994). Activation of dynamin GTPase is a result of positive cooperativity. J. Biol. Chem. *269*, 30842–30847.

Tuma, P.L., Stachniak, M.C., and Collins, C.A. (1993). Activation of dynamin GTPase by acidic phospholipids and endogenous rat brain vesicles. J. Biol. Chem. *268*, 17240–17246.

Urrutia, R., Henley, J.R., Cook, T., and McNiven, M.A. (1997). The dynamins: redundant or distinct functions for an expanding family of related GTPases? Proc. Natl. Acad. Sci. USA *94*, 377–384.

van der Bliek, A.M., and Meyerowitz, E.M. (1991). Dynamin-like protein encoded by the Drosophila *shibire* gene associated with vesicular traffic. Nature *351*, 411–414.

van der Bliek, A.M., Redelmeier, T.E., Damke, H., Tisdale, E.J., Meyerowitz, E.M., and Schmid, S.L. (1993). Mutations in human dynamin block and intermediate stage in coated vesicle formation. J. Cell Biol. *122*, 553–563.

Vieira, A.V., Lamaze, C., and Schmid, S.L. (1996). Control of EGF receptor signaling by clathrin-mediated endocytosis. Science *274*, 2086–2089.

Volchuk, A., Narine, S., Foster, L.J., Grabs, D., De Camilli, P., and Klip, A. (1998). Perturbation of dynamin II with an amphiphysin SH3 domain increases GLUT4 glucose transporters at the plasma membrane in 3T3-L1 adipocytes. J. Biol. Chem., *273*, 8169–8176.

Warnock, D.E., and Schmid, S.L. (1996). Dynamin GTPase, a force-generating molecular switch. BioEssays *18*, 885–893.

Warnock, D.E., Hinshaw, J.E., and Schmid, S.L. (1996). Dynamin self-assembly stimulates its GTPase activity. J. Biol. Chem. *271*, 22310–22314.

Warnock, D.E., Baba, T., and Schmid, S.L. (1997). Ubiquitously expressed dynamin-II has a higher intrinsic GTPase activity and a greater propensity for self-assembly than neuronal dynamin-I. Mol. Biol. Cell *8*, 2553–2562.

Zheng, J., Cahill, S.M., Lemmon, M.A., Fushman, D., Schlessinger, J., and Cowburn, D. (1996). Identification of the binding site for acidic phospholipids on the PH domain of dynamin: implications for stimulation of GTPase activity. J. Mol. Biol. *255*, 14–21.